Equilibrium Geometry and Properties Of Cyclo[(Gly-D-Ala)4] and {Cyclo[(Gly-D-Ala)4]}2 from Density Functional Theory

R. A. Jishi,[†] R. M. Flores,[†] M. Valderrama,[†] L. Lou,[‡] and J. Bragin*[,§]

Department of Physics, California State University, Los Angeles, California 90032, Wavefunction, Inc., 18401 Van Karman, Irvine, California 92715, and Department of Chemistry, California State University, Los Angeles, California 90032

Cyclic peptides containing even numbers of alternating D- and L-amino acids adopt a symmetric ring structure with NH and CO amide functions approximately perpendicular to the average plane of the ring. This results in hydrogen-bonded, β-sheet like tubular ensembles by coaxial stacking of rings in which adjacent strands are oriented antiparallel to one another. Starting from a molecular mechanics minimum energy configuration having the C_4 symmetry reported for similar structures, an optimized monomer geometry which retained that symmetry was obtained using density functional theory (DFT). The geometry of the monomer is quite similar to that of stable polypeptides and proteins and the calculated gas-phase harmonic vibrational frequencies are quantitatively reasonable. Two monomers were then brought together coaxially, with adjacent strands arranged antiparallel, creating a dimer of D_4 symmetry. Dimer energy was then minimized with respect to ring separation along, and relative rotation of one ring with respect to the other about, the common C_4 axis. The interstrand separation in this dimer model is reasonable in comparison with experimental values reported for stable β-sheet polypeptides and proteins as are the harmonic vibrational frequencies. An approximation to the harmonic N−H···O stretching frequency calculated for this dimer model was also physically reasonable by comparison to the interchain motion calculated for β-sheet polypeptides from analysis of experimental vibrational frequencies. Though synthesis of the molecules in this study has not been reported, they serve as excellent models for the analysis of ring structure and for isolating the role of backbone−backbone hydrogen bonds in the stacking process for similar assemblies. This study provides theoretical support for experimental work on more complex systems, and the DFT calculations are among the largest ever for the study of molecular systems using double valence single polarization basis sets.

1. Introduction

Tubular structures of molecular dimensions have attracted considerable attention lately. Carbon nanotubes, as well as other nanotubes containing boron and nitrogen have been produced by the arc-discharge method.[1−6] Furthermore, filling of carbon nanotubes by a variety of other materials has been demonstrated experimentally,[7−11] raising the possibility of applications in nanoelectronics and reaction chemistry.

Recently, a new class of organic nanotubes has been reported[12−17] in which open ended hollow tubular units are formed by the self-assembly of flat ring-shaped polypeptide subunits. Naturally occurring peptide and protein-based tubular structures are well-known. Examples include tobacco mosaic virus, bacterial pili, and the antibiotic gramicidin A. However, the rational design strategies that have been developed to construct the synthetic assemblies allow production of a wide range of tubular structures with specific pore diameters and surface characteristics. Such materials could have an extraordinarily wide range of applications from transmembrane channels for drug delivery into living cells to development of devices with unique optical or electronic properties.

Nanotubes self-assembled from rings containing even numbers of alternating D- and L-amino acids are remarkably stable

in a variety of harsh chemical and physical environments. Such cyclic polypeptides adopt (or sample) a flat ring shaped structure in which the backbone amide functions, N−H and C═O, lie approximately perpendicular to the plane of the structure and are oriented to form continuous, hydrogen bonded, β-sheet like tubular ensembles by coaxial stacking of individual rings. Furthermore, conformational and steric constraints imposed by the alternating amino acid backbone configuration position the amino acid side chains outward, away from the ring backbone. This creates a hollow, amphiphilic pore and provides a means to engineer the surface properties of the tubular assemblies for a variety of biological and materials science applications in which the physical and chemical properties of the medium in which the tubes are imbedded are critical. Recent studies have also demonstrated that these same backbone features greatly favor antiparallel ring stacking and homochiral cross strand nearest neighbor pairing or registration of the peptide units of adjacent strands.[17] Such an arrangement makes for an exceedingly tight fit as the rings stack and introduces a 2-fold rotation axis perpendicular to the principal axis.

In this work we report first-principles calculations, within the density functional theory, of the equilibrium structure and electronic properties of cyclo[(Gly-D-Ala)4], as well as two of its dimers {cyclo[(Gly-D-Ala)4]}2. Though the experimental synthesis of the particular peptide ring studied in this work has not been reported, yet it serves as an excellent model for the

---

[†] Department of Physics.
[‡] Wavefunction, Inc.
[§] Department of Chemistry.

Cyclo[(Gly-D-Ala)₄] and {Cyclo[(Gly-D-Ala)₄]}₂

J. Phys. Chem. A, Vol. 102, No. 48, 1998 **9859**

study of ring structure, and for isolating the role of backbone—backbone hydrogen bonds in the stacking process in more complex systems with larger numbers of amino acids per ring, and larger, chemically active amino acid side groups. The initial experimental work with cyclopeptides utilized systems with carboxylate-containing side chains as pH sensitive triggers for self-assembly.[13] This introduced the possibility of a substantial cross strand side chain side chain contribution to the self-assembly energetics. Subsequent work demonstrated that when such groups are absent interstrand registration is not sensitive to cross strand side chain—side chain interactions.[17] Furthermore, ab initio geometry optimization has been largely confined to very small model systems.[18] While a few applications of DFT to such problems have been reported,[19] most have not used full basis sets.[20] This work represents a significant expansion in both respects and provides theoretical support for the ideas that have guided the experimental work of Ghadiri et al.[12–17]

2. Computational Methods

The DFT calculations performed in this study take advantage of three-dimensional numerical integrations[21] which allow for atomic orbital basis functions in the place of conventional Gaussian type orbitals. The numerical basis sets consist of a single function for each core electron and two functions for each valence electron. The minimum set is obtained from a solution of the ground state of the corresponding atom. The split valence subset is obtained by solving a 2+ ionic state of the same atom (for hydrogen, a bare nucleus of charge $Z = 1.3$ is used, instead). Polarization functions are added to both the heavy atoms and the hydrogen atoms. For C, N, and O, the 3d hydrogenic orbital of N^{7+} is used, and for H, the 2p orbital of He^{2+}. These numerical solutions preserve the nuclear cusps, the radial nodal positions, and the exponentially decaying tail of an atomic wave function, which all help to reduce errors caused by basis set incompleteness.

The optimization of the structure is carried out in two steps. First, a molecular force field calculation is performed[22] to determine the starting geometry of the molecule. Then, a DFT calculation is performed using the program CMOL[23] to further relax the atomic positions. The relaxation is terminated when the maximum force on an atom is less than 0.001 atomic units. The corrections to the exchange and correlation energy[24] are included in a post self-consistent gradient-field manner. The deviation thus caused in binding energy from a full self-consistent treatment is of the order of a few tenths of kcal/mol, in the worst case tested. This should be considered satisfactory given a reduction in cost by 3—4 times.

The cyclopeptide dimer contains 136 atoms and requires a total of 1328 basis functions in the DFT calculations. This is among the largest problems solved at the ab initio level of theory with polarized basis sets on both heavy atoms and hydrogen. The computations were performed on an SGI Origin 200 equipped with dual MIPS 10000 processors, and the computer program has been parallelized to better support calculations in this size range.[25] Calculations were also performed on the U.S. Naval Research Laboratory's SGI Origin 2000 using 8 or 16 MIPS 10 000 processors. The DFT calculation of the vibrational frequencies of the monomer took about 350 h on the Origin 200.

The size of the molecules in the present study results in a prohibitively time-consuming DFT calculation for the Hessian matrix. As an alternative, we used a semiempirical method, MOPAC93/PM3,[26] to perform the vibrational frequency calculation for the dimer and recalculated the frequencies of the
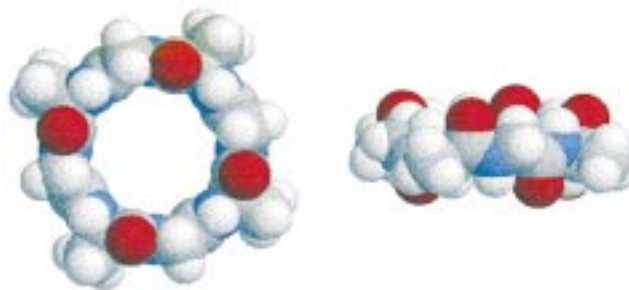
Figure 1. DFT-optimized geometry for cyclo[(Gly-D-Ala)₄]. (Oxygen = red, nitrogen = blue, carbon = gray, hydrogen = white.) Top view of the 68-atom space-filling representation of the cyclic peptide with C_4 symmetry. Side view showing the flat ring shaped structure in which N—H and C=O lie approximately perpendicular to the average plane of the backbone.

monomer at this level of approximation as well. To be consistent, all the molecular structures were relaxed at this level of theory and the Hessian matrix elements evaluated at the new minimum energy geometry.

3. Results and Discussion

A. Monomer. The optimized structure for the monomer is shown in Figure 1 and its geometrical parameters given in Table 1. The bond lengths and angles of both residues are quite similar and little different from the standard peptide geometry. The conformational parameters (torsional angles) of the D-alanine residues are quite similar to those found in open chain β-sheets. Conformational restrictions on glycine are relaxed due to the absence of a side-chain but the structure found is well within the regions of stability in the Ramachandran map[27] for this peptide.

The peptide link is quite close to being planar and well within the range of observed deviations in ω from the planar trans value (180°). This is consistent with the findings that the bond lengths and angles show barely any departure from the standard geometry and supports the view that there is little or no strain in this structure. Harmonic vibrational frequencies have been calculated for the gas phase monomer and are quantitatively reasonable given the expected shifts due to anharmonicity and intermolecular interaction. Eight N—H stretching modes are calculated in the range 3421 to 3453 cm⁻¹ (Amide A), twenty-four C—H stretches are calculated in the range 2911 to 3056 cm⁻¹, and eight Amide I modes (C=O stretch) are calculated in the 1718 to 1744 cm⁻¹ range (Table 2). The atomic displacements of the other normal modes are not as localized in a specific chemical functional group.

Computed harmonic frequencies for the monomer are not strictly comparable to observed anharmonic frequencies measured in solution. Vibrational frequencies obtained from electronic structure calculations can be as much as 12% above experimental values due to the use of the harmonic approximation to the vibrational potential energy and the failure to take electron correlation fully into account.[28] Such effects are clearly shown in the PM3 values of the Amide I vibrational frequencies in Table 2. Even nonoxygenated solvents such as CHCl₃ interact strongly enough with amides to introduce a 2 kcal/mol decrease in the enthalpy of self-association of N-methylacetamide, a solute—solvent interaction energy comparable to the strength of N—H⋯O hydrogen bonds.[29] Below 10⁻² M, the solubility limit of these species in inert solvents, even traces of water absorbed from the atmosphere can interfere as well. Furthermore, the spectra calculated in this work do not include

TABLE 1: Geometric Parameters in Monomeric Cyclo[(Gly-D-Ala)$_4$]

		DFT		PM3		standard geometry[b]
		Gly[a]	D-Ala[a]	Gly[a]	D-Ala[a]	
bond lengths (angstroms)	C=O	1.23	1.23	1.23	1.23	1.23
	C−N	1.34	1.34	1.40	1.39	1.32
	N−H	1.03	1.02	1.00	1.00	1.00
	N−C$^\alpha$	1.43	1.44	1.48	1.47	1.47
	C$^\alpha$−C	1.50	1.51	1.53	1.54	1.53
bond angles (degrees)	C$^\alpha$CN	117	117	118	118	114
	C$^\alpha$CO	120	119	123	123	121
	NCO	123	124	119	119	
	C$^\alpha$NC	121	120	121	120	123
	C$^\alpha$NH	116	116	117	119	
	CNH	123	124	121	122	123
angles of C=O and N−H bond dipoles with Cartesian axes (degrees); z is C_4 symmetry axis	C=O					
	x	91, 87	86, 93	91	86	
	y	93, 91	87, 86	93	87	
	z	180	6.5	179	6.5	
	N−H					
	x	102, 97	97, 90	102	97	
	y	83, 101	90, 97	83	90	
	z	166	7.2	166	7.1	

		DFT		PM3		antiparallel β-poly(L-Ala)[d]
torsional angles (degrees)[c]		Gly[a]	D-Ala[a]	Gly[a]	D-Ala[a]	
torsional angle about N−C$^\alpha$	ϕ	−141	144	−141, −146	143	−138.4
torsional angle about C$^\alpha$−C	ψ	141	−138	141	−133, −138	136.7
torsional angle about N−C	ω	178, 176	178, 176	177	178	180

[a] This work. Geometric parameters changed by 1% or less on dimerization resulting in contact through either the D-alanine or glycine faces. There is a small difference in the z direction cosines of the carbonyl bond dipole in both dimers (Gly = 175°, D-Ala = 4.6°). [b] Corey, R. B.; Pauling, L. *Proc. R. Soc. London, Ser. B.* **1953**, *141*, 10−20. [c] IUPAC−IUB Commission on Biochemical Nomenclature. *Biochemistry* **1969**, *9*, 3471. [d] Arnott, S.; Dover, S. D.; Eliott, A. *J. Mol. Biol.* **1967**, *30*, 201−208. (The regions of stability in the Ramachandran plane for enantiomers are reversed.)

TABLE 2: Calculated Vibrational Frequencies (cm^{-1}) for Some Polypeptides

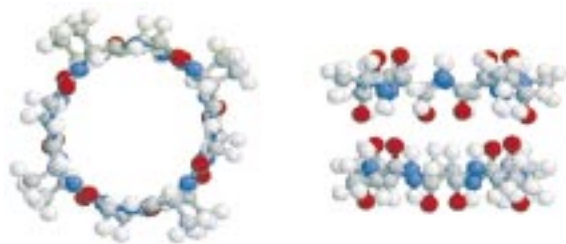|	cyclo[(Gly-D-Ala)$_4$][b]				
	monomer		dimer		
vibrational assignment[a]	DFT	PM3[d]	PM3[d]	β-polyGly(I)[c]	β-poly(L-Ala)[c]
N−H str	3421−3453	3359−3382	3355−3368	3271	3242
C−H str	2911−3056	2833−3185	2825−3181	2861−2934	2864−2984
Amide I	1718−1744	1876−1886	1860−1882	1643−1695	1630−1698
Amide II, III	?−1526	1462−1502	1462−1502	1286−1602	1299−1592
		1274−1297	1272−1295		
		1229−1240	1227−1240		
HCH, HCC def	936−1428	1395−1410	1392−1405	940−1454	969−1455
		1355−1359	1353−1359		
		1312−1338	1309−1337		
		1244−1248	1247−1253		
		1205−1212	1209−1214		
		1113, 1139	1104−1140		
		1044−1065	1043−1063		
		956−962	955−963		
C$^\alpha$−C$^\beta$ str	e	1103−1108	1102−1109		1054−1205
C$^\alpha$−N str	e	1064−1137	1044−1141	1014−1213	913−1198
C$^\alpha$−C	e	990−993	989−997	767−890	788−913
		883−898	882−898		
Amide IV	e	701−774	706−775	629, 630	624−628
Amide V	e	405−476	424−491	702−736	704−708
CH$_3$ torsions	e	181−191	186−197		238−240
backbone def	e	<660	<665	<622	<627

[a] str = stretch, def = deformation. The Amide I−VII modes are assigned by analogy with those calculated from a fit to the experimental vibrational frequencies of *N*-methylamide using a general valence force field.[30] Amide I−IV are motions in the plane of the peptide group. Amide I is principally C=O stretching, Amides II and III are out-of-phase and in-phase combinations of the NH deformation and CN stretching motions, respectively, and Amide IV is a combination of C=O deformation and C$^\alpha$C stretching. Amide V−VII are out-of-plane motions. Amide V and VII are largely NH deformation and Amide VI is a C=O deformation. [b] This work. Geometry optimized in the regime used to calculate the vibrational frequencies. Glycine faces in contact in dimer. [c] Calculated from a fit to experimental frequencies using a general valence force field unique for each peptide.[30] [d] From MOPAC93.[26] [e] Signifies that characterization of these normal modes in terms of group frequencies or internal coordinates is uncertain based only on the calculated nuclear displacements in Cartesian coordinates.

terms for Fermi resonance and transition dipole coupling which have been demonstrated to split observed Amide A, I, and II bands by amounts comparable to or greater than that produced by the general quadratic force field used here.[30]

Cyclo[(Gly-D-Ala)4] and {Cyclo[(Gly-D-Ala)4]}2

J. Phys. Chem. A, Vol. 102, No. 48, 1998 **9861**
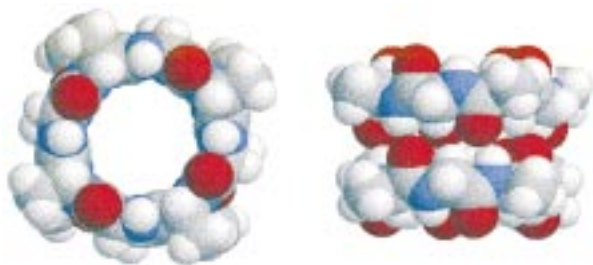
Figure 2. DFT-optmized geometry for {Cyclo[(Gly-D-Ala)4]}2, D-Alanine faces in contact.]. (Oxygen = red, nitrogen = blue, carbon = gray, hydrogen = white.) Top view of the space-filling representation of the dimer with D_4 symmetry and one ring rotated 8° with respect to the other. Side view of the dimer showing the orientation of the hydrogen-bonded N−H and C=O groups.

Figure 3. DFT-optimized geometry for {cyclo[(Gly-D-Ala)4]}2, Glycine faces in contact. (Oxygen = red, nitrogen = blue, carbon = gray, hydrogen = white.) Top view of the ball-and-stick representation of the dimer with D_4 symmetry and one ring rotated 8° with respect to the other. Side view of the dimer showing the orientation of the hydrogen bonded N−H and C=O groups.

The harmonic frequencies of the monomer computed in the DFT level of theory in this study can be considered to represent an upper limit to the frequencies of the normal modes of the free peptide group and are comparable to the value 3470 cm^{-1} observed for the NH stretching mode in *N*-methylacetamide vapor and the value 1708 cm^{-1} for the Amide I mode in the trans *N*-methylacetamide monomer in a frozen Argon matrix.[31] On the other hand, since the Amide II mode (predominantly CNH deformation) shifts upward on association,[29] it is expected that the calculated harmonic frequency range for this mode in the free monomer will fall below the experimental value in peptide nanotubes as observed.[12,16]

B. Dimer. The dimer was constructed by bringing together two identical cyclic polypeptide monomers along the *z* axis perpendicular to the plane of the rings. To obtain the preferred antiparallel relationship of the juxtaposed strands, one was rotated by 180° around an axis perpendicular to *z* resulting in a dimer complex of D_4 symmetry. Only two parameters were adjusted in the dimerization process: the distance between the rings or interstrand separation, as measured by the mean difference in *z* coordinates of the backbone N and C atoms, and the relative rotation of one ring with respect to the other around their common *z* axis (ring registration). The minimum energy conformation found is shown in Figures 2 and 3 for the configuration in which the D-alanine and glycine faces are in contact, respectively. Some important geometric parameters for the two dimers are given in Table 3.

To more fully characterize the hydrogen bond, we have plotted the dimerization energy calculated by the DFT method with gradient corrections to the exchange and correlation energies[24] as a function of interstrand distance as measured by the average difference in backbone C and N atoms in Figure 4. The open circles represent the DFT energies calculated as described in the preceding section. These points have been fit

TABLE 3: Geometric Parameters for Some Antiparallel β-Pleated Sheets

		{Cyclo[(Gly-D-Ala)4]}2[a]		
		D-Ala/ D-Ala	Gly/ Gly	β-poly-(L-Ala)[b]
bond lengths (angstroms)	N···O	3.12	2.96	2.83
	H···O	2.17	2.01	1.75
bond angles (degrees)	HNO	17.5	18.3	9.8
	NHO	154	152	164.6
interstrand separation (angstroms)		4.97	4.82	4.73

[a] This work from DFT calculations. D-Alanine/D-alanine or glycine/glycine cross strand interactions. [b] Arnott, S; Dover, S. D.; Eliott, A. *J. Mol. Biol.* **1967**, *30*, 201−208.
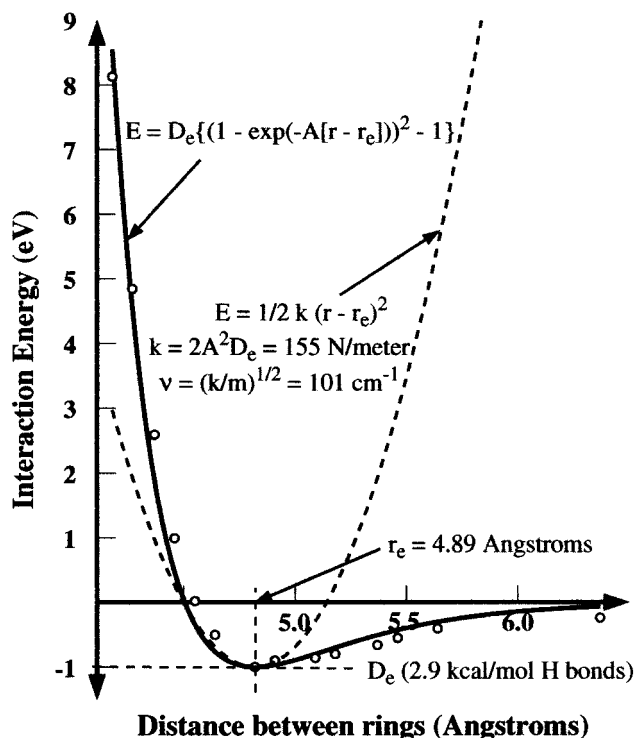
Figure 4. Dimerization energy as a function of monomer separation along the *z* figure axis. Glycine faces in contact. Open circles represent the results from the DFT calculations for the dimer and were used to fit the Morse potential function (solid curve). D_e is the equilibrium dissociation energy adjusted during the fitting process. *r* is the interstrand separation defined as the mean difference in *z* coordinates of the backbone N and C atoms. r_e is the equilibrium interstrand separation adjusted during the fitting process. *k* is the Hooke's law force constant evaluated from the curvature of the Morse potential at the equilibrium point. m is the reduced mass of the N−H···O vibrational mode of the dimer. *A* is an adjustable scaling parameter.

to a Morse potential by adjusting the parameters D_e and r_e, respectively, the dissociation energy and interstrand separation measured at the equilibrium interstrand separation. *A* is an adjustable scaling parameter. The minimum corresponds to a separation of 4.89 Å in good agreement with the value found for other β-pleated sheets and remarkably close to experimental values for several similar cyclopeptide nanotubes with a variety of side chains.[12−15] The DFT dimerization energy for this configuration is 1.0 eV (2.9 kcal per mol of H bonds).

The curvature of the Morse potential function at the equilibrium interstrand separation, $2A^2D_e$, is then set equal to the Hooke's law force constant for the N−H···O hydrogen bond stretch and a frequency of 101 cm^{-1} calculated from the reduced mass for this mode of vibration. This value is in reasonable agreement with a Raman band observed at 112 cm^{-1} in

antiparallel β-pleated rippled sheets of polygly(I) and the value of 135 cm^{-1} calculated for the totally symmetric N−H···O stretching frequency from an analysis of the vibrational frequencies of this material.[30]

The relative orientation of the rings in the dimer was also varied in order to find the lowest energy structure. To obtain the lowest energy structure, one ring was rotated in relation to the other, so that the vector connecting corresponding atoms in each ring was not parallel to the C_4 axis (z axis). A vector joining the C$^\alpha$ atoms of two adjacent glycine units or two adjacent alanine units makes a small angle of approximately 7° with the C_4 axis at the minimum energy. This rotation, which is most clearly illustrated in Figure 2, demonstrates the preference for nearly exact homochiral cross strand registration.

Since the ab initio calculation of dimer vibrational frequencies was prohibitively time-consuming on available computing machinery the geometry of the monomer and dimers was re-optimized in the PM3 approximation and frequencies calculated with the program MOPAC93. A comparison of these results and the monomer frequencies calculated in the DFT regime is shown in Table 2 along with an analysis of experimental frequencies of some β-pleated sheets. The semiempirical calculations are not particularly sensitive to the affect of hydrogen bond formation on the N−H stretching frequency, although they do show a slight downward shift. The affect of hydrogen bond formation on the PM3 Amide I frequencies is comparable to that resulting from Hartree−Fock calculations on N-methylacetamide.[31]

Results of Hartree−Fock calculations support the suggestion that a cooperative effect acts to strengthen the hydrogen bond in N-methylacetamide polymers where both N−H and C=O groups in the molecule are hydrogen bonded.[31] A 10% increase in hydrogen bond strength, a 0.005−0.006 Å decrease in C−N, a 0.004−0.005 Å increase in C=O, and a 20 cm^{-1} decrease in the Amide I frequency were found when the N-methylacetamide molecule participates in a second hydrogen bond. Thus the 2.9 kcal/mol hydrogen bond energy found here for the dimer in which only half of each peptide group is involved in hydrogen bonding may represent a lower limit to the hydrogen bond energies in peptide nanotubes.

References and Notes

(1) Ijima, S. *Nature* **1991**, *354*, 56.
(2) Ebbesen T. W.; Ajayan, P. M. *Nature* **1992**, *358*, 220.
(3) Ijima S.; Ichihashi, T. *Nature* **1993**, *363*, 603.
(4) Bethune, D. S.; Klang, C. H.; Devries, M. S.; Gorman, C.; Savoy, R.; Vasquez, J.; Byers. R. *Nature* **1993**, *363*, 605.
(5) Thess, A.; Lee, R.; Nikolaev, P.; Dai, H.; Petit, P.; Robert, J.; Xu, C.; Lee, Y. H.; Kim, S. G.; Rinzler, A. G.; Colbert, D. T.; Scureria, G. E.; Tomanek, D.; Fischer, J. E.; Smalley, R. E. *Science* **1996**, *273*, 483.
(6) Chopra, N. G.; Luyken, R. J.; Cherrey, K.; Crespi, V. H.; Cohen, M. L.; Louie, S. G.; Zettl, A. *Science* **1995**, *269*, 966.
(7) Loiseau, A.; Williame, F.; Demoncy, N.; Hug, G.; Pascard, H. *Phys. Rev. Lett.* **1996**, *76*, 4737.
(8) Ajayan, P. M.; Iijima, S. *Nature* **1993**, *361*, 333.
(9) Ajayan, P. M.; Ebbesen, T. W.; Ichihashi, T.; Iijima, S.; Tanigaki, K.; Hiura, H. *Nature* **1993**, *362*, 522.
(10) Guerret-Piecourt, C.; Le Bouar, Y.; Loiseau, A.; Pascard, H. *Nature* **1994**, *372*, 159.
(11) Dujardin, E.; Ebbesen, T. W.; Hiura, H.; Tanigaki, K. *Science* **1994**, *265*, 1850.
(12) Ghadiri, M. R.; Granja, J. R.; Milligan, R. A.; McRee, D. E.; Khazanovich, N. *Nature* **1993**, *366*, 324.
(13) Ghadiri, M. R. Granja,; J. R.; Buehler, L. K. *Nature* **1994**, *369*, 301.
(14) Khazanovich, N.; Granja, J. R.; McRee, D. E.; Milligan, R. A.; Ghadiri, M. R. *J. Am. Chem. Soc.* **1994**, *116*, 6100.
(15) Ghadiri, M. R.; Kobayashi, K.; Granja, J. R.; Chadha, R. K.; McRee, D. E. *Angew. Chem., Int. Ed. Engl.* **1995**, *34*, 93.
(16) Hartgerink, J. D.; Granja, J. R.; Milligan, R. A.; Ghadiri, M. R. *J. Am. Chem. Soc.* **1996**, *118*, 43.
(17) Kobayashi, K.; Granja, J. R.; Ghadiri, M. R. *Angew. Chem., Int. Ed. Engl.* **1995**, *34*, 93.
(18) Cieplak, P.; Cornell, W. D.; Bayly, C.; Kollman, P. A. *J. Comput. Chem.* **1995**, *16*, 1357. Morwell, D. S.; Tuodo-Rives, J.; and Jorgensen, W. L. *J. Comput. Chem.* **1995**, *16*, 984.
(19) Carloni, P.; Andreoni, W.; Parrinello, M. *Phys. Rev. Lett.* **1997**, *79*, 761.
(20) Takeda, K.; Shiraishi, K. *J. Phys. Soc. Jpn.* **1996**, *65*, 421. Gailar, C.; Feigel, M. *J. Comput.-Aided Mol. Des.* **1997**, 11, 273. Lewis, J. P.; Pawley, N. H.; Sankey, O. *J. Phys. Chem. B* **1997**, *101*, 10576.
(21) Becke, A. D. *J. Chem. Phys.* **1988**, *88*, 2547. Delley, B. *J. Chem. Phys.* **1991**, *92*, 508.
(22) Brooks, B. R.; Bruccoleri, R. E.; Olafson, B. D.; States, D. J.; Swaminathan, S.; Karplus, M. *J. Comput. Chem.* **1983**, *4*, 187.
(23) Lou, L.; Nordlander, P.; Smalley, R. E. *J. Chem Phys.* **1992**, *97*, 1858.
(24) Vosko, S. H.; Wilk, L.; Nusair, M. *Can. J. Phys.* **1980**, *58*, 1200. Becke, A. D. *Phys. Rev. A.* **1988**, *38*, 3098. Perdew, J. P. *Phys. Rev. B.* **1986**, *35*, 9822.
(25) Lou, L.; Nordlander, P.; Smalley, R. E. *Phys. Rev. B.* **1995**, *52*, 1429.
(26) Stewart, J. J. P. *J. Comput. Chem.* **1989**, *10*, 209, 221.
(27) Ramachandran, G. N.; Sasisekharan, O. *Adv. Protein Chem.* **1968**, *23*, 283.
(28) Hehre, W. J.; Radom, L.; Schleyer, P. V. R.; Pople, J. A. *Ab Initio Molecular Orbital Theory*; J. Wiley & Sons: New York, 1986.
(29) Pimentel, G. C.; McClellan, A. L. *The Hydrogen Bond*; W. H. Freeman and Co.: San Francisco, 1960.
(30) Krimm, S.; Bandekar, J. *Adv. Protein Chem.* **1986**, *38*, 188.
(31) Torii, H.; Tatsumi, T.; Kanazawa, T.; Tasumi, M. *J. Chem. Phys. B.* **1998**, *102*, 3.